Statics and Dynamics of ω-Functionalized Block Copolymers of Styrene and Isoprene

G. Floudas* and G. Fytas

Foundation for Research and Technology (FORTH)—Hellas, Institute of Electronic Structure and Laser, P.O. Box 1527, 711 10 Heraklion, Crete, Greece

S. Pispas† and N. Hadjichristidis†

Department of Chemistry, University of Athens, Panepistimiopolis, Zografou 15771, Athens, Greece

T. Pakula

Max-Planck-Institut für Polymerforschung, Postfach 3148, D-55021 Mainz, FRG

A. R. Khokhlov

Department of Physics, Moscow State University, Moscow 117234, Russia

Received January 13, 1995; Revised Manuscript Received April 25, 1995⊗

ABSTRACT: The statics and dynamics of ω-functionalized diblock copolymers of styrene and isoprene have been studied with small-angle X-ray scattering (SAXS) and with rheology and dielectric spectroscopy. The asymmetric diblock copolymers ($w_{PS} \approx 30\%$) had a dimethylamino or zwitterion group at either end of the chain, and the molecular weights were in the range $(0.62-2.44) \times 10^4$. Depending on the temperature, the SAXS results revealed two separate levels of microphase separation, one between the polystyrene (PS) and polyisoprene (PI) blocks forming the microdomain structure and another one between ionic and nonionic material. The latter process creates sufficient contrast notwithstanding the small fraction of the zwitterionic groups. When the zwitterion is linked to the PI chain end, aggregates are formed at low temperatures within the PI phase. These aggregates manifest themselves both in rheology and in dielectric spectroscopy, respectively, with an extended rubbery plateau and with a new dielectric process associated with restricted PI segmental relaxation. When the zwitterion is located on the PS chain end, association takes place, at high temperatures, within the PS phase and acts to stabilize the new microdomain up to very high temperatures. When compared with neutral diblocks, the ω-functionalized diblock copolymers constitute a new class of materials which provide the possibility of altering the phase behavior by introducing a small amount of a polar group at one chain end.

Introduction

Ion-containing polymers are materials with unique physical properties which have attracted extensive experimental and theoretical work. These materials are hydrocarbon polymers containing ionic groups which are discussed as ionomers[1–3] (usually less than 10%) or polyelectrolytes[4] (more than 10%). The first studies on ionomers were made with random ionomers,[1,2] where the ionic groups were randomly distributed along the polymer chain. Ionic groups are more polar than the hydrocarbon chains, and this creates an electrostatic driving force for association which normally exceeds the elasticity of polymer chains and results in the formation of ionic aggregates. There is consensus that such ionic aggregates are responsible for the unique physical properties of ionomers. Evidence for ionic aggregation exists in (i) the small-angle X-ray and neutron scattering patterns[5] with the new "ionomer peak" and (ii) from rheology[6,7] and dielectric spectroscopy[8] with the extension of the rubbery plateau and the existence of a new loss peak at higher temperatures. Different structural models[9–11] have been proposed, aiming to describe these results, but a detailed structural description in terms of size, shape, internal structure, and spatial organization is still missing. This ambiguity originates mainly from the limited structure in the SAXS patterns which show only a single and broad scattering peak.

A better understanding of the morphology and structure in ion-containing polymers can be brought about by studying model compounds where the position of ionic groups can be controlled. Telechelic ionomers,[12,13] where the ionic groups are located at the chain ends and block copolymer ionomers,[14–17] where one of the blocks is ionized, are two classes of such model compounds which recently have attracted attention. The latter system exhibits an interesting three-phase microstructure with ionic aggregates dispersed within one of the block copolymer domains.

The association behavior of end-functionalized polyisoprenes with the highly polar zwitterion group has been studied by SAXS[18] and rheology,[19,20] both in solution and in the melt. The SAXS study[18] from the lower molecular weight PI melts revealed the formation of two-dimensional lattices of close-packed aggregates where the core was made up of the zwitterionic heads. For the higher molecular weights (MW > 14 000), the aggregates formed a body-centered cubic lattice with long-range order. The rheological investigation[20] revealed an extended aggregate structure for the zwitterion phase. This was supported by the enhancement of the viscosity—being larger than for a starlike structure—and from the anomalous strain dependence at low frequencies. The synthesis and dilute solution properties of ω-functionalized diblock and triblock copolymers of styrene and isoprene with one dimethylamino or zwitterionic group at either or both ends of the chain have only recently been reported.[21,22]

† Also at FORTH.

⊗ Abstract published in *Advance ACS Abstracts,* June 15, 1995.

0024-9297/95/2228-5109$09.00/0

Table 1. Molecular Characteristics of the ω-Functionalized Styrene–Isoprene Diblock Copolymers

sample	$10^{-4}\bar{M}_w$[a]	$10^{-4}\bar{M}_n$[b]	$\bar{M}_w/\bar{M}_n$[c]	% PS[d] (w/w)	%, 3,4[d] vinyl	%, 1,2[d] vinyl	T_g^{low} (K)	T_g^{high} (K)
NIS-6	0.62	0.51	1.19	16	38	3		
NIS-8	0.91	0.83	1.1	27	28		229	
NIS-5	1.41	1.22	1.06	28	20		226	
NIS-4	1.79	1.57	1.07	29	18.5		226	
NIS-3	2.44	2.25	1.07	28	17			
NSI-8	1.14	1.04	1.1	32	57	6	269	
NSI-5	1.49	1.34	1.11	32	63	12	270	313–345
NSI-4	1.88	1.7	1.08	30	59	13	256	319–347

[a] Low-angle laser light scattering. [b] Membrane osmometry. [c] Size-exclusion chromatography. [d] ^{1}H-NMR.

In the present investigation, we employ the same ω-functionalized diblocks to study the static and dynamic response in the melt state and access the end-group association effects. For this purpose we use SAXS to study the level of spatial organization and rheology and dielectric spectroscopy to infer the consistency of the local segmental and global dynamics with morphology in a series of asymmetric ($w_{PS} \approx 30\%$) SI diblocks with molecular weights in the range from 0.62×10^4 to 2.44×10^4. We find, in general, two levels of microphase separation: one between the PS and PI blocks (microdomain) and another between the polar and nonpolar material (association). The association produced by the latter process affects both the rheological and dielectric responses of the system. The introduction of a polar group into the different chain ends produces a dramatic change on the phase behavior of the system.

Experimental Section

Polymer Synthesis. The ω-functionalized block copolymers of styrene (S) and isoprene (I) were prepared, under high-vacuum conditions, in all-glass reactors provided with break seals for the addition of reagents and constrictions for removal of products.[23,24] The dimethylamino functionality was introduced to either the polyisoprene (PI) or the polystyrene (PS) chain end by polymerizing the appropriate monomer first using [3-(dimethylamino)propyl]lithium as the initiator.[19,25,26] Living ends were terminated with degassed methanol at the end of the second polymerization. The basic reactions are schematically the following:

$$\text{S (or I)} + Me_2N(CH_2)_3Li \rightarrow Me_2N(PS)Li \text{ [or } Me_2N(PI)Li\text{]} \quad \text{(A)}$$

$$\text{(A)} + \text{I (or S)} \rightarrow Me_2N(PS)(PI)Li \text{ [or } Me_2N(PI)(PS)Li\text{]} \quad \text{(B)}$$

$$\text{(B)} + MeOH \rightarrow \text{NSI (or NIS)}$$

The conversion of the amine-capped block copolymers to the sulfozwitterion ones was achieved by reaction with cyclopropanesultone according to the following scheme:

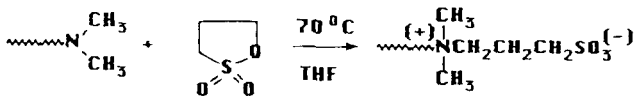

More details for the synthetic procedure are given elsewhere.[21]

Size-exclusion chromatography (THF, 30 °C), low-angle laser light scattering (THF, 25 °C), membrane osmometry (toluene, 30 °C), and ^{1}H-NMR ($CDCl_3$, 30 °C) measurements were performed by following procedures published elsewhere.[27,28] The characteristics of the amino-capped precursors are given in Table 1.

SAXS Measurements. The small-angle X-ray measurements were made with a Kratky Compact camera (A. Paar, KG) equipped with a one-dimensional position-sensitive detector (M. Braun). The Ni-filtered Cu Kα radiation ($\lambda = 0.154$ nm) was used from a Siemens generator (Kristalloflex 710H) operating at 35 kV and 30 mA. A special furnace was constructed which served as the sample holder, and all measurements were made under vacuum. Measurements of 1 h duration were made in intervals of 5 K within the range 298–423 K, with a stability better than ±0.2 K. Changes between successive temperatures were completed within 3 min and a 30-min waiting time was preset for equilibration. The intensity data at a scattering vector of magnitude Q ($=(4\pi/\lambda)\sin(\theta/2)$, where θ is the scattering angle) up to 3 nm^{-1} were collected in a multichannel analyzer and transferred to a Vax station for further analysis. Data treatment involved correction for absorption, background scattering, and slit-length smearing. Primary beam intensities were determined—in absolute units—by using the moving slit method. Our earlier studies[29–31] on block copolymers have shown that local concentration fluctuations as well as density fluctuations are present in the SAXS background. For a reliable subtraction the temperature dependence of the isothermal compressibility β_T is needed. In the present study, we do not measure directly $\beta_T(T)$ but we have used the measured $\beta_T(T)$ from asymmetric SI block copolymers of similar molecular weights.

Dielectric Spectroscopy. The real and imaginary parts of the complex dielectric permittivity ε* were measured for the sample Zw-SI#4 in the frequency range 10^{-1}–10^5 Hz with a frequency response analyzer (Solartron Schlumberger 1260) in the temperature range 263–363 K. For the rest of the samples a Hewlett-Packard HP 4284A impedance analyzer was used in the frequency range 20–10^6 Hz and for temperatures within 238–427 K. Samples were kept between two gold-plated stainless steel electrodes of 20 mm diameter with a separation of 50 mm being maintained by fused silica spacers. The sample temperature was adjusted by a jet of temperature-controlled nitrogen gas with a stability better than ±0.1 K. The dielectric data have been fitted to the empirical equation of Havriliak–Negami (HN):

$$\epsilon^*(\omega) = \epsilon_\infty + \frac{\epsilon_0 - \epsilon_\infty}{[1 + (i\omega\tau_{HN})^\alpha]^\gamma} \qquad 0 < \alpha, \gamma < 1 \qquad (1)$$

where $\Delta\epsilon = \epsilon_0 - \epsilon_\infty$ is the relaxation strength of the process under investigation which is given by the difference between the low- and high-frequency values of the real part of the dielectric permittivity and τ_{HN} is the characteristic relaxation time of this equation. The parameters α and γ, respectively, describe the symmetrical and asymmetrical broadening of the distribution of relaxation times. The steep rise at low frequencies is caused by the electrical conductivity within the sample, which has been fitted by $\epsilon'' = (\sigma_0/\epsilon_f)\omega^{-1}$, where σ_0 is a fitting parameter and ϵ_f is the permittivity of free space.

Rheology. The storage and loss moduli G' and G'' were measured with a Rheometrics RMS800 in the oscillatory mode and with a parallel-plate sample geometry. The frequency used was 1 rad/s, and the temperature varied from 200 to 450 K.

DSC. Differential scanning calorimetry was used to identify the glass transition temperatures of the end-functionalized SI block copolymers. Samples were first cooled to 120 K at a rate of 20 K/min and subsequently heated to 423 K at 15 K/min. The same procedure was repeated for a second heat with a rate of 10 K/min. For all samples a very broad high T_g could be resolved which corresponds to the T_g of the PS block. The

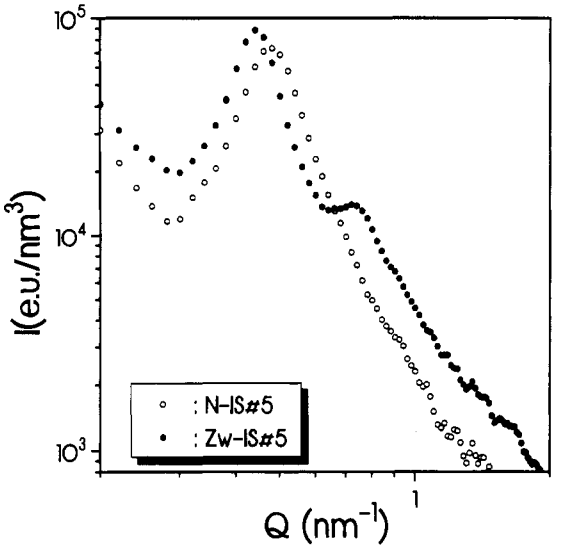

Figure 1. SAXS profiles for two ω-functionalized IS diblock copolymers at $T = 303$ K. Data have been corrected for the density fluctuations (see text), and the intensities are given in absolute units. Notice that the high Q peak due to ionic aggregation is only present in the zwitterion-substituted copolymer Zw-IS.

Chart 1

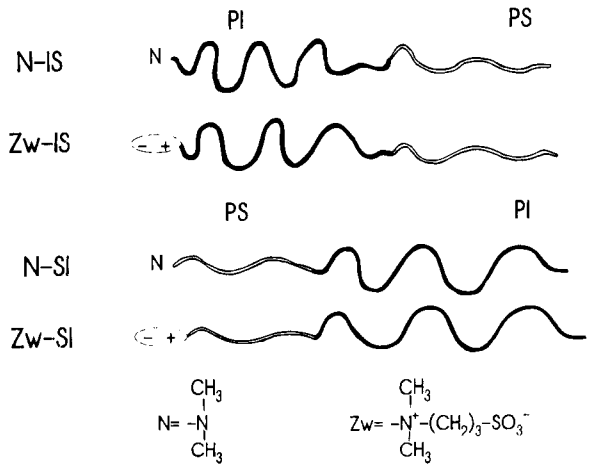

T_g values obtained from the first run for the SI copolymers with the dimethylamino and zwitterionic end groups are given in Table 1.

Data Analysis

A typical SAXS pattern of an SI diblock copolymer with a dimethylamino end group (N-IS#5) is shown in Figure 1 at 303 K. The scattering pattern is dominated by a peak in $S(Q)$ at a position Q^* which is characteristic of the size of the system. Judging from the high peak intensity and the narrow line width—as compared to the $S(Q)$ at higher T—we conclude that the peak in $S(Q)$ at 303 K is related to the microphase separation which takes place between the PS and PI phases and creates sufficient scattering contrast. The microstructure—based on the styrene content—is that of hexagonally packed cylinders with a spacing of $d_{mic} = 134$ Å, organized in domains with a thickness of $D \approx 500$ Å calculated from the peak position and width, respectively. From the position of the first Bragg maximum and some simple geometrical considerations we can calculate the cylinder radius

$$R_c = d_{mic}\left(\frac{\sqrt{3}}{2\pi} f_{PS}\right)^{1/2} \quad (2)$$

which is equal to 35 Å for N-IS#5.

In addition to the microdomain peak, there is an increased scattering at small Q which, however, is not related to the isothermal compressibility and therefore to the density fluctuations within the material. The latter can be calculated from the isothermal compressibility β_T ($=-1/V(\partial V/\partial P)_T$)[29,30]

$$I(0) = \tilde{n}^2 k_B T \beta_T(T) \quad (3)$$

where $\tilde{n}$ is the average electron density. It is worth noticing that although $\beta_T(T)$ is not expected to be greatly affected by the presence of the zwitterionic end groups, the level of density fluctuations (defined by $\langle \delta N^2 \rangle / \langle N \rangle \approx I(0)$, where δN is the fluctuation of the number of particles N) will increase in the presence of polar groups as a result of the increase in $\tilde{n}$ (see below). In the following, we have corrected the SAXS spectra using the measured $\beta_T(T)$ from the neutral SI diblock copolymers and used eq 3 to subtract the contribution of the density fluctuations at each temperature.

The remaining excess intensity at small Q shows a systematic change with molecular weight (see Figure 5, below) and functionality and implies a connection with the distribution of ionic groups. Due to the limited Q range a characteristic correlation length (using the Debye–Bueche theory) cannot be unambiguously extracted from the data on hand. We should point out, however, that excess low-Q intensities exist even in single component systems at temperatures much higher than the calorimetric T_g, and this feature has been associated with long-range density fluctuations discussed by Fischer et al.[32] The excess intensity in the case of ionomers[11,12,33] has been discussed in terms of heterogeneities with a length scale longer than the characteristic distance between aggregates.

When the dimethylamino group is replaced by the zwitterionic group there are distinct changes in the SAXS pattern. This is shown in Figure 1 where the SAXS pattern for N-IS#5 is compared with the one from Zw-IS#5. The position of the microdomain peak shifts to smaller Q (with a corresponding cylinder spacing of 139 and a radius of 36 Å), retaining its shape, but at a larger Q a second peak appears with a smaller intensity. This second peak, which appears only for block copolymers with polar end groups originates from a microphase separation between the ionic and nonionic material. There are two different ways to envision this kind of phase separation, which depends on the balance between the electrostatic interactions of the polar groups and the elastic forces of the chains. The first is more appropriate at low T and involves the formation of aggregates composed of polar groups. In the second picture, there is a delicate balance between the elastic forces and the electrostatic interactions which can stabilize a structure in which the polar end groups are distributed between the cylinders formed by PS within the PI matrix (see Figure 9, below). Notwithstanding the small fraction of ionic material, in both pictures, there is sufficient contrast because of the great electron density difference between the two phases. It is expected that the two structures will differ in their rheological and dielectric response (see below). Our experimental results (see below) rule out the possibility of ionic groups located near the PS–PI interphase.

The integrated spectral intensity offers a means of calculating the size of aggregates. For an ideal two-phase system, that is, a mixture composed of ionic and nonionic phases where the boundary shows a sharp transition from high to low-electron density, the scattering invariant P

$$P = \frac{1}{2\pi^2}\int_0^\infty I(Q)\, Q^2\, dQ \tag{4}$$

depends on the relative amounts of the two phases ϕ and $1 - \phi$ and on the electron density difference:

$$P = \phi(1 - \phi)(n_1 - n_2)^2 \tag{5}$$

Equation 5 can be generalized for a system containing three phases as

$$P = \phi_1\phi_2(n_1 - n_2)^2 + \phi_1\phi_3(n_1 - n_3)^2 + \phi_2\phi_3(n_2 - n_3)^2 \tag{6}$$

where the subscripts 1–3 refer to PI, PS, and ionic aggregates, respectively. The first term in eq 6 refers to the microdomain peak, while the remaining two refer to the ionic peak. To deconvolute the two sources of scattering we have fitted the two peaks in the IQ^2 vs Q representation and estimated the related intensities. For the electron densities of PI and PS at 303 K we have used 301 and 340 electrons/nm^3, respectively. To calculate the electron density of the ionic phase we have assumed: (i) complete segregation between the two phases and (ii) additivity of group molar volumes and compared with the density of cyclopropanesultone ($n_{agg} \approx 379$ electrons/nm^3). On the basis of these assumptions we obtain the volume fraction of ionic domains $\phi_3 = \phi_{agg} \approx 0.044$.

Results and Discussion

Static Structure. The comparison (Figure 1) between the dimethylamino- and zwitterion-functionalized diblocks (N-IS and Zw-IS) clearly shows that ionic aggregation is taking place only in the latter system. Assuming spherical aggregates ($R_{agg} = ((3d_{agg}/4\pi)\phi_{agg})^{1/3}$) with $\phi_{agg} = 0.044$ and $d_{agg} = 8.2$ nm for Zw-IS#5, we obtain an estimate for the radius R_{agg} of ionic domains of about 5 Å, which corresponds to the size of zwitterions attached to the PI block. This estimate of the radius of aggregates is in good agreement with that of functionalized linear polyisoprenes using the same zwitterionic functionality.[18] There, a tubelike structure for the dipolar head groups was proposed with antiparallel configurations which minimize the electrostatic interactions. The temperature dependence of the SAXS pattern for Zw-IS#5 is shown in Figure 2 for temperatures in the range 303–383 K. All three characteristic features of the scattering pattern, namely, the intensity at small Q, the microdomain peak, and the peak due to ionic aggregation, display a significant T dependence. The microdomain peak changes from a narrow peak (ordered state) to a much broader peak at high T (disordered state). With increasing T, both peaks move to higher Q, which is a characteristic feature of block copolymers near but below the microphase separation temperature.[30,31,34] Notice, however, that there is no clear evidence for the T_{ODT} from the spectra shown in Figure 2. In a recent SAXS study[35] on sulfonated poly[styrene-*b*-(ethylene-*co*-butylene)-*b*-styrene] (SSEBS) such a transition has been observed.

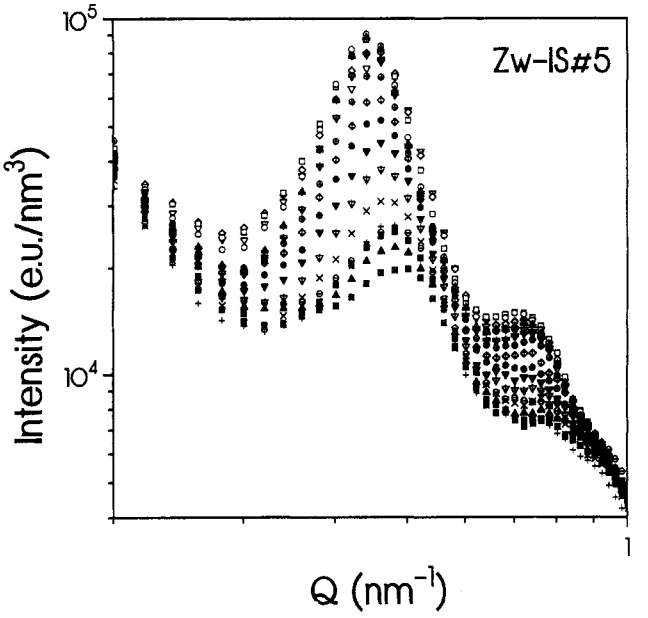

Figure 2. Temperature dependence of the SAXS profile for the Zw-IS#5 sample (MW = 14 100, w_{PS} = 28%). Data are shown within the temperature range 303–383 K in steps of 5 K. For the first four temperatures (▽) 303, (◇) 308, (□) 313, (○) 318 K) the intensity increases with T as a result of the increasing contrast between the PS and PI phases below the PS glass transition.

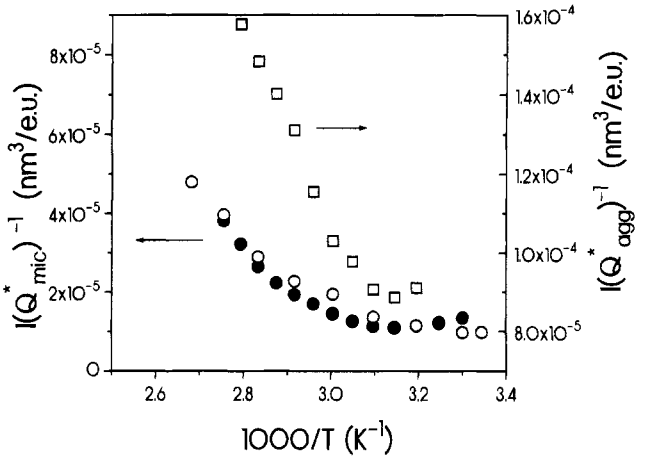

Figure 3. Inverse peak intensity vs inverse temperature for the microdomain $I(Q_{mic}^*)$ (●) and ionic peaks $I(Q_{agg}^*)$ (□) of Zw-IS#5. The temperature dependence of the microdomain peak in N-IS#5 (○) is also shown for comparison.

The intensities of both peaks for Zw-IS#5 are plotted in Figure 3 as a function of inverse temperature. The copolymer microdomain peak intensity, $I(Q_{mic}^*)$, changes by about 60% whereas the aggregate peak intensity, $I(Q_{agg}^*)$ only by 36%, within the same temperature range. Furthermore, there is a pronounced nonlinearity in the plot of $I(Q_{mic}^*)^{-1}$ vs T^{-1}, and this has been discussed in terms of fluctuation effects which are important for the rather small molecular weights MW of our copolymers. The microdomain peak intensity of N-IS#5 is also plotted in Figure 3 and displays a T dependence similar to that of the corresponding Zw-IS. In Figure 4 we plot the peak position for the two peaks in Zw-IS as a function of temperature. The T dependence of the microdomain peak, Q_{mic}^*, is reminiscent of linear block copolymers: it increases linearly with T for $T > T_{g,high}$ and is continuous throughout the transition. Notwithstanding the different T dependence of the

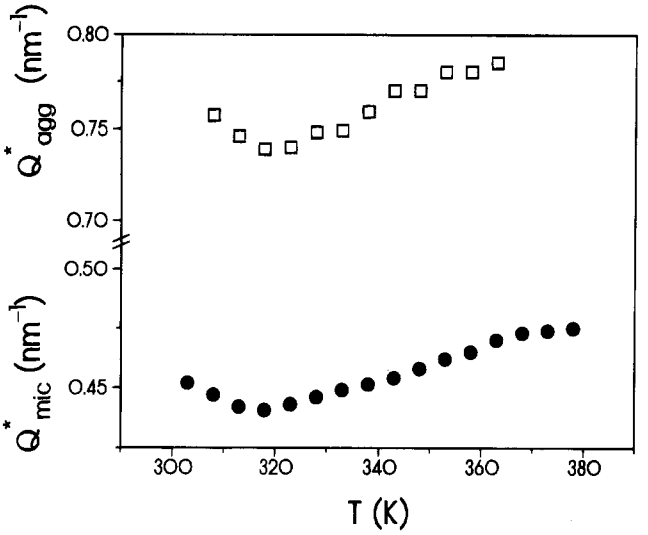

Figure 4. Temperature dependence of the two peaks shown in Figure 1 for Zw-IS#5.

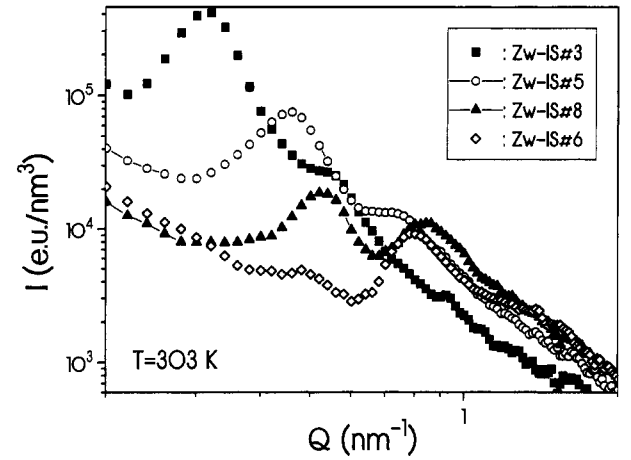

Figure 5. MW dependence of the SAXS profiles for the zwitterionic-functionalized IS copolymers (Zw-IS) plotted at 303 K. The weight fraction of PS is 28% except for Zw-IS#6 (w_{PS} = 16%).

intensity, the peak position, Q_{agg}*, follows that of the microdomain peak. In conclusion, the microdomain and ionic structures are interrelated: both peak positions and intensities display a T dependence.

The MW dependence of the scattering profiles has also been studied for the samples shown in Table 1. The SAXS patterns for the Zw-IS samples with MW in the range 6.2×10^3–2.4×10^4 are shown in Figure 5. All spectra display three features: (i) an excess intensity at small Q, (ii) a microdomain peak, and (iii) an ionic peak, but the relative intensity among the three depends strongly on the MW. Decreasing the MW results in an increase of the relative intensity of the ionic peak since the volume fraction of ionic domains increases. For the lower MW investigated (Zw-IS#6) the SAXS pattern is dominated by the aggregation peak since only a small peak due to the "correlation hole" effect exists. Increase of MW affects not only the relative intensities but also the positions of both peaks. In general, increasing the MW has the same effect as decreasing T; both peaks move to smaller Q values. It is this increase in d_{agg} ($=2\pi/Q_{agg}$*) which balances the reduction of the volume fraction ϕ_{agg} and produces a MW-independent size for the ionic domains. The MW dependence for both peaks is shown in a double logarithmic plot in Figure 6, at a

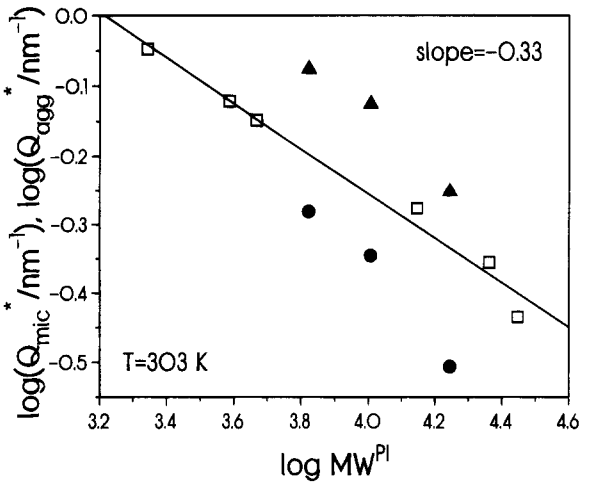

Figure 6. MW dependence of the scattering vector corresponding to the microdomain (●) and ionic (▲) peak positions for the Zw-IS samples at T = 303 K. The solid line is a fit to the literature data (□) for the ω-functionalized linear polyisoprenes, and the slope is −0.33.

common temperature (T = 303 K). Data from the lower MW sample are excluded since the w_{PS} for this sample is low (16%). The MW dependence of the ionic peak in linear ω-functionalized PIs with the same polar group (zwitterion) is also shown. The SAXS investigation[18] of the ω-functionalized PIs has shown that for low molecular weights a lattice is formed with cylindrical symmetry but for higher molecular weights (MW ≥ 1.4×10^4) there was a transition to a cubic lattice. From Figure 6, $d_{agg} < l < d_{mic}$ where l is the characteristic spacing in the case of the functional PIs. Taking into account the cylinder radius and the size of the polar head group, we find that the PI chain is slightly contracted in the case of Zw-IS in comparison to Zw-I, or in other words, the PI chain is less extended in the former system. The expectation is, however, that in the vicinity of the PS cylinders the PI chains are stretched and this is also true in the vicinity of the ionic aggregates. The PI chain ends which are organized in the aggregates repel from the cylinders to have as much entropy as possible for aggregation. A line with a slope of −0.33 is also drawn through the PI data but the data for the diblocks are not linear probably because of the different phase state (disordered vs ordered) of the materials at this temperature. We mention here, parenthetically, that a slope of −0.33 signifies ionic domains of constant density since their size was found to be independent of MW.

When the zwitterion functionality is linked to the polystyrene chain end (Zw-SI), a different behavior is displayed in the SAXS profiles (Figures 1 and 7). The scattering pattern is now dominated by the microdomain peak which has gained in intensity when compared to the corresponding Zw-IS samples (Figure 1). With increasing T, the microdomain peak sharpens; from a domain size of 600 Å at 303 K the size increases to about 900 Å at 393 K and the peak position moves slightly to higher Q. A pertinent feature of the SAXS pattern for all Zw-SI samples is the absence of any dissolution of the microdomain structure with increasing T within the T range of our experiment. This finding is in sharp contrast to the situation with the Zw-IS samples and with the corresponding dimethylamino SI copolymers (N-SI) and is illustrated in Figure 8 where the SAXS pattern of Zw-SI#5 is compared with the corresponding data for N-SI#5 at two temperatures.

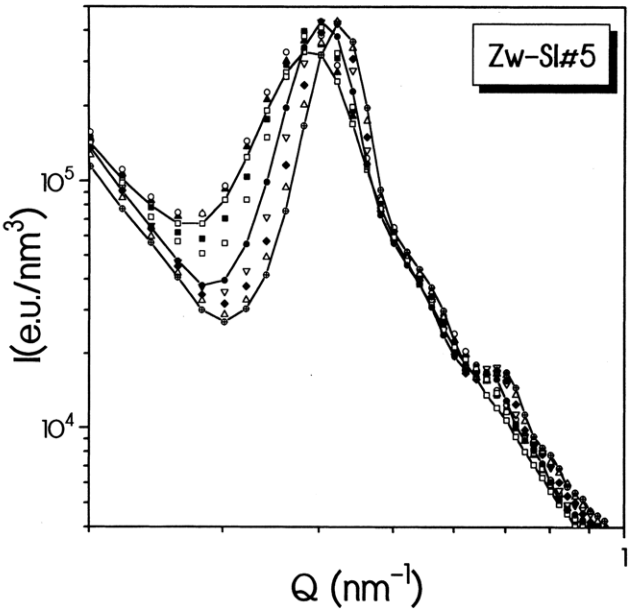

Figure 7. SAXS profiles for the zwitterion-functionalized SI copolymer ZW-SI#5 (MW = 14 900, w_{PS} = 32%) at some selected temperatures in the range 298 (□) to 423 (⊕) K.

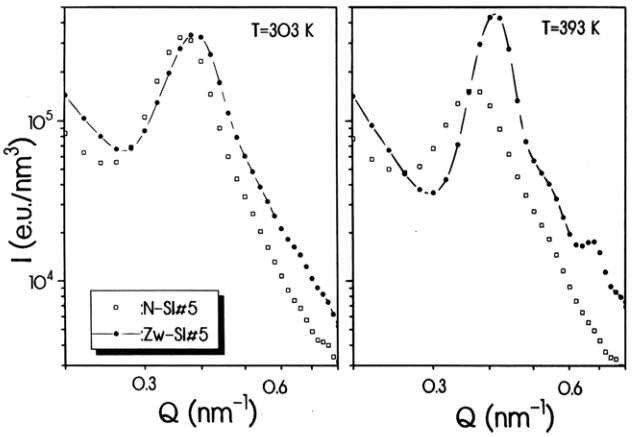

Figure 8. Comparison of the SAXS profiles for the dimethylamino- and zwitterion-substituted ω-functionalized copolymers at two temperatures as indicated.

The microdomain structure is clearly stabilized (increased incompatibility) by the zwitterionic group substitution on the PS chain end. This brings forward a new possibility of altering the phase behavior of diblock copolymers. Until recently, drastic changes in the phase diagram of block copolymers required alteration of the molecular architecture.[36,37] The fact that one can change substantially the phase behavior by substituting a very small amount of polar groups can have a great scientific and technological importance.

With increasing temperature, the structure of Zw-SI becomes better defined with additional peaks at positions corresponding to $2^{1/2}$ and $3^{1/3}$ of the main peak position. This implies a transition to a cubic (simple or body centered) structure. This is illustrated schematically in Figure 9 for the Zw-IS and Zw-SI systems for the different temperature regimes. In the Zw-SI system, and for $T < T_g^{PS}$ depending on the thermal history, the functional groups are trapped within the immobile PS phase without being able to aggregate. With increasing T, more of the polar groups find sufficient mobility to overcome the elastic forces and lower the electrostatic interactions, forming ionic aggregates within

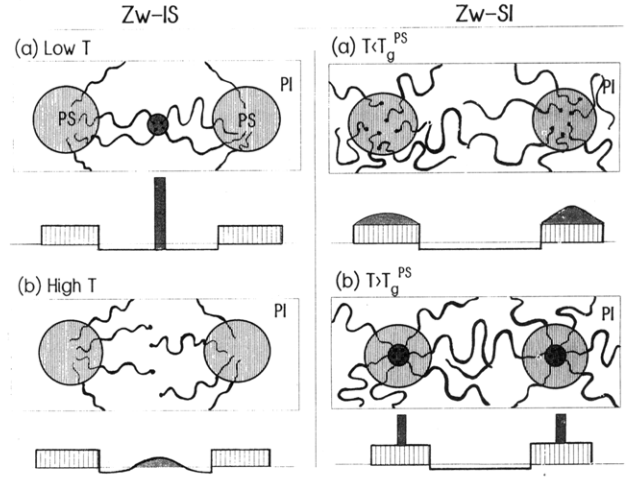

Figure 9. Schematic illustration of the microstructures in ω-functionalized SI block copolymers, showing the Zw-IS (left) and Zw-SI (right) cases at low (upper) and high (lower) temperatures. The corresponding electron density distributions are also shown.

the "hard" phase. This kind of transition is in agreement with the SAXS results shown in Figures 7 and 8. These aggregates act to stabilize the new microdomain structure which is consistent with the fact that the order increases with T (Figure 8). There is consensus that ionic aggregation takes place in the medium with the low dielectric constant *and* low T_g. The dielectric constant of PS ($\epsilon_{PS} = 2.49-2.55$) is similar to that of PI ($\epsilon_{PI} = 2.37-2.45$) and, notwithstanding the higher T_g of PS, ionic aggregation in Zw-SI is taking place within the PS phase. On the other hand, if the aggregates were formed consistently in the mobile phase (PI), then we could interpret neither our SAXS data shown in Figures 7 and 8 nor the results from the dynamic studies (below).

Dynamic Response. The static measurements on the ω-functionalized SI block copolymers revealed two types of microphase separation: (i) between PI and PS blocks which gives rise to the usual microdomain peak in the structure factor of block copolymers and (ii) between ionic and nonionic material which gives rise to some new features in $S(Q)$. The phase in which aggregation takes place depends on whether the polar end group is attached to the hard (PS) or soft (PI) polymer. This kind of twin microphase separation makes the ω-functionalized SI copolymers an interesting system for studying the effect of confinement on the local and global chain dynamics. For this purpose we employ rheology and dielectric spectroscopy, with the former being selective to the PI chain.

The dynamic mechanical measurements were made at a single (low) frequency over a broad temperature range, and the storage and loss moduli of N-SI#4 and Zw-SI#4 samples are shown in Figure 10, along with the loss tangent. In general, a microphase-separated diblock copolymer is expected to show four relaxations. Starting from low temperatures: (i) PI segmental relaxation, (ii) PI block relaxation, (iii) PS segmental relaxation, and (iv) PS block relaxation and/or relaxation of the aggregation as a whole. Additionally, a sudden drop of the moduli is expected[30,31,34] for low frequencies at the order-to-disorder transition which results from a transition from a solid- to a liquid-like state. Figure 10 shows four relaxations (better seen in the loss tangent) for both samples. The low-T peak in tangent δ is associated with the PI segmental relaxation

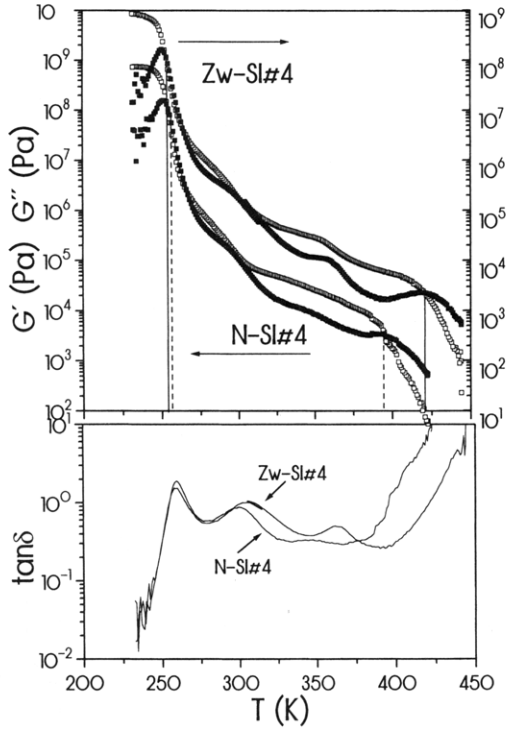

Figure 10. Temperature dependence of the storage (open symbols) and loss (filled symbols) moduli at $\omega = 1$ rad/s for the ω-SI#4 copolymers. The loss tangent ($=G''/G'$) is also shown.

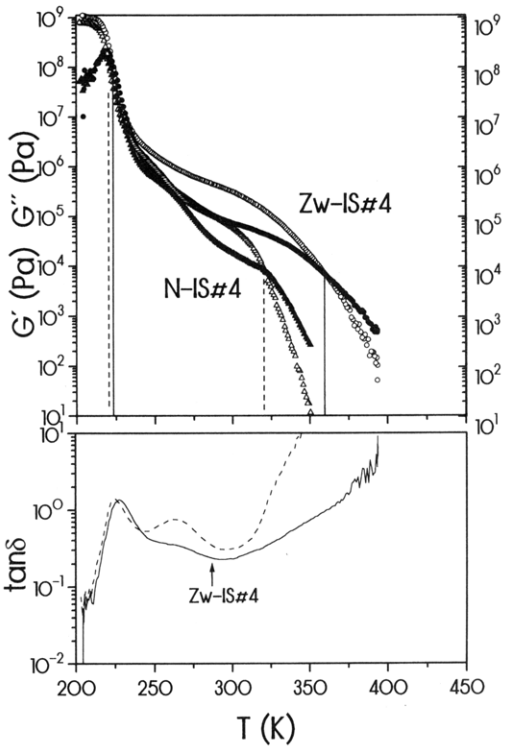

Figure 11. Temperature dependence of the storage (open symbols) and loss (filled symbols) moduli at $\omega = 1$ rad/s as well as of the loss tangent for the end-functionalized block copolymers ω-IS#4 with the dimethylamino and zwitterion group.

and is in good agreement with the T_g^{PI} obtained from DSC. The relatively high T_g as compared with other polyisoprenes is explained by the higher 3,4 vinyl content for both samples (Table 1). The second peak exists in both N-SI#4 and Zw-SI#4 samples and is slightly shifted to higher T in the latter. The third peak is much more pronounced in Zw-SI#4 and clearly shifted to higher T which may signify an increase in the glass transition of PS. For the functionalized Zw-SI copolymers, ionic aggregation takes place within the PS phase (Figure 9) which stabilizes the microdomain structure over an extremely broad temperature range. The fourth relaxation clearly shifts to higher T in Zw-SI#4 which reflects the fact that hindrance of the PS block relaxation is due to the presence of aggregates. In addition, this relaxation could also correspond to the flow of the structure as a whole in a manner similar to that of large star molecules. Ionomers also show a high-T loss peak which has been associated with the ionic structure. The storage modulus shows an extension of the plateau which is reminiscent of the plateau in cross-linked systems.[7] The extension of the rubbery plateau in the case of ionomers has been discussed in terms of the ionic cross-linking produced by the aggregates and/or of the aggregates acting as reinforcing filler particles. The same arguments can also be used for the present system. Within the temperature range investigated there is no indication for an order-to-disorder transition from $G'(T)$, which is in agreement with the SAXS results and supports a stabilized cubic microdomain structure up to very high temperatures.

When the functional group is placed on the PI chain end (N-IS and Zw-IS) the dynamic mechanical response of the system is altered. In Figure 11, we plot the storage and loss moduli of N-IS#4 and Zw-IS#4 at $\omega =$ 1 rad/s as a function of T. The low-T peak in the loss tangent is again associated with the I segmental relaxation and occurs at lower T than for the samples shown in Figure 10, because of the smaller 3,4 vinyl content of the PI block. Furthermore, this low-T relaxation in N-IS#4 is only slightly shifted by the zwitterionic end group. A pertinent feature in Figure 11 is the suppression of the second peak in Zw-IS#4. There are two effects which can account for this suppression. First, the PI block relaxation can be significantly suppressed by the fixing of PI chain ends to the PS cylinders from one side and to the ionic aggregates from the other. Since the aggregates are formed in the mobile phase, only partial subchain relaxation can occur that causes the suppression in Figure 11. Second, this peak may be associated with a new process originating from PI segments of reduced mobility in the neighborhood of polar aggregates. In this picture, aggregates act as large cross-links which reduce the mobility of PI and create a higher T_g, which shows up in the dynamic mechanical spectra as a peak of reduced amplitude. The above two alternatives are likely to be interrelated, and to differentiate between the two would require dynamic measurements over a broad frequency range. For this purpose we will use below dielectric spectroscopy which selectively probes the PI chain. Like the situation in the Zw-SI system (Figure 10), the terminal zone in Zw-IS is shifted by 40 K to higher T when compared to N-IS (Figure 11), notwithstanding the similar molecular weight for both samples. The extension of the rubbery plateau in the former constitutes evidence for the existence of ionic aggregates which act as cross-links and favors the SAXS picture at low T (Figure 9). At high T ($T > 360$ K) the rheological response becomes terminal, corresponding to a new structure where the polar end groups are arranged between the PS cylinders with a liquid-like order (Figure 9).

In Figure 12, we compare the storage and loss moduli for three Zw-IS copolymers with MW in the range 0.91

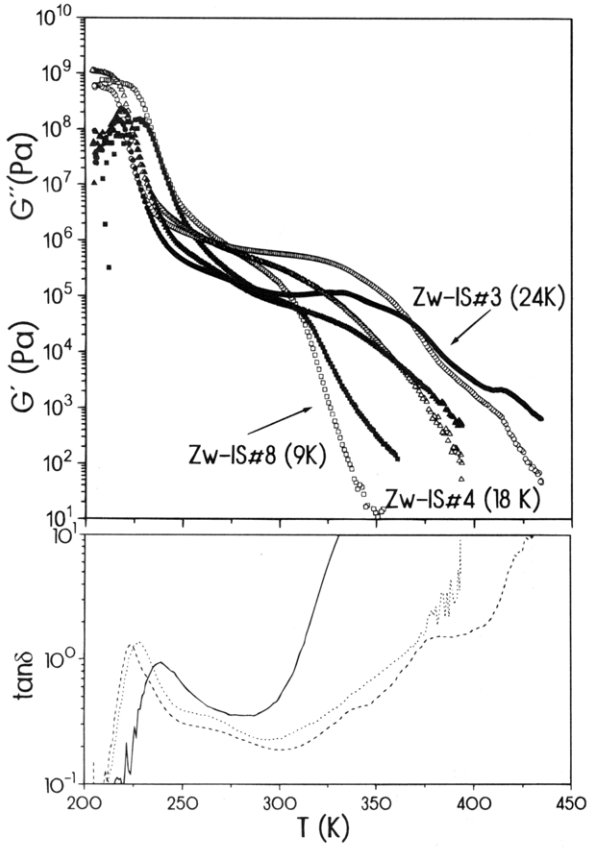

Figure 12. Storage (open symbols) and loss (filled symbols) moduli for three ω-functionalized block copolymers Z-IS with total molecular weights in the range 0.91×10^4 to 2.44×10^4, plotted as a function of temperature at 1 rad/s.

$\times 10^4$–2.44×10^4. A second peak with suppressed amplitude exists in all samples. Moreover, the terminal relaxation is shifted by more than 50 K. It is interesting to note the different slopes at high T which reflect the existence or absence of the microdomain structure. The high T data for the smaller MW (Zw-IS#8) display a liquid-like behavior with the associated single chain dynamics. For this MW, the T_{ODT} is expected to be coupled to the polystyrene T_g and at $T > T_g^{PS}$ mainly the ionic structure exists (Figure 9). Notice that the phase mixing is also evident in the PI-like segmental motion which is shifted to higher T. The dynamic picture above agrees with the SAXS pattern (Figure 5) which shows a rather small peak due to the microdomain or from the correlation hole scattering. On the other extreme, for the Zw-IS#3 sample the microdomain structure dominates (Figure 5) and changes only moderately with T up to 383 K. The viscoelastic response above 400 K is quite complex. The weak T dependence of G' and G'' in the temperature range 375–410 K is reminiscent of diblock copolymers near but below the T_{ODT}. However, at higher T there is no clear evidence for the order-to-disorder transition. It may be that the temperature range where the transition occurs is enlarged or that the transition is smeared out. The T dependence of Zw-IS#4 is intermediate between the ones discussed. In conclusion, the rheological response of the Zw-IS samples is affected by the presence of the microdomain structure in addition to the ionic structure.

From the dynamic mechanical measurements made at a single frequency it was difficult to comment on the origin of the suppressed second peak in the data shown in Figures 11 and 12. With dielectric spectroscopy, however, we can study the dynamics at much higher

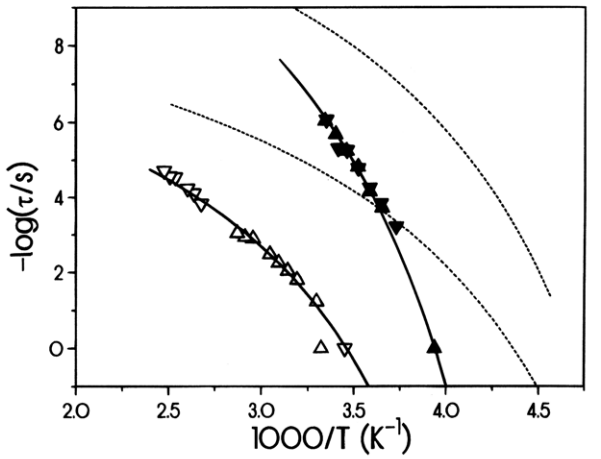

Figure 13. Arrhenius plot of the normal (open symbols) and segmental (filled symbols) relaxation times for Zw-SI#4 (▲, △) and N-SI#4 (▼, ▽) in comparison with bulk PI (dashed line). Solid lines are fits to the VFT.

frequencies provided that the system has sufficient dielectric contrast. PS has only a weak dipole moment perpendicular to the chain but PI has two components, one perpendicular and the other along the main chain. The perpendicular component is sensitive to rapid local motions (segmental mode) whereas the parallel component (normal mode) provides information on the slow dielectric response involving fluctuations of the end-to-end polarization vector of the chain.[38,39] In the absence of cross-correlations among the chain dipoles the complex dielectric constant ϵ^* of the normal mode process can be expressed by the Fourier–Laplace transform of the autocorrelation function $\langle \mathbf{r}(0)\cdot\mathbf{r}(t)\rangle/\langle r^2\rangle$ of the end-to-end vector:

$$\frac{\epsilon^*(\omega) - \epsilon_\infty}{\Delta\epsilon} = \frac{1}{\langle r^2\rangle}\int_0^\infty \exp(-i\omega t)\left(-\frac{\mathrm{d}\langle \mathbf{r}(0)\cdot\mathbf{r}(t)\rangle}{\mathrm{d}t}\right)\mathrm{d}t \quad (7)$$

For nonentangled linear chains the free-draining model proposed by Rouse gives[40]

$$\langle \mathbf{r}(0)\cdot\mathbf{r}(t)\rangle = \frac{8\langle r^2\rangle}{\pi^2}\sum_{p_{odd}}\frac{1}{p^2}e^{-t/\tau_p} \quad (8)$$

with

$$\tau_p = \frac{\zeta N^2 b^2}{3\pi^2 k_B T}\frac{1}{p^2} \qquad p\text{: odd} \quad (9)$$

where τ_p is the relaxation time of the pth normal mode and ζ is the monomeric friction coefficient. For nonentangled bulk polymers this equation becomes

$$\tau_p = \frac{12M\eta}{\pi^2\varrho RT}\frac{1}{p^2} \quad (10)$$

where η is the zero-shear viscosity, M is the molecular weight, and ϱ is the density. According to the Rouse model the relaxation time is proportional to M^2.

The dielectric data for the segmental and normal modes have been consistently fitted to the HN equation (eq 1), and the relaxation strength ($\Delta\epsilon$), the shape parameters (α, γ), and the characteristic relaxation time (τ_{HN}) have been obtained. From these parameters we extract the relaxation time τ_{max} which is plotted in an Arrhenius representation in Figure 13 for Zw-IS#4 and

N-SI#4. The segmental and normal modes of bulk PI with a comparable MW are also shown in Figure 13. All relaxation processes have been fitted to the Vogel–Fulcher–Tammann (VFT) equation:

$$\log \tau = \log \tau_0 + \frac{B}{T - T_0} \tag{11}$$

where τ_0, B, and T_0 are characteristic parameters which describe the high-T intercept, the apparent activation energy, and the "ideal" glass transition temperature, respectively. The parameters log τ_0, B, and T_0, assume the following values for the segmental and normal modes, respectively, in bulk PI: −13 and −8.96, 590 and 585 K, 168 and 164 K.

As expected, the segmental relaxation times for the ω-SI copolymers with the dimethylamino and zwitterionic functionalities are indistinguishable and this is borne out by the local character of this process. When compared to the segmental relaxation of bulk PI, this process is shifted to higher T in the ω-functionalized copolymers as a result of the different 3,4 vinyl content. Furthermore, the single dynamic mechanical relaxation time is in good agreement with the dielectric times from higher T. The normal mode process is also shifted to higher T, but this is a composite effect owing to the change of the local segmental friction and to an additional retardation resulting from fixing one PI end on the PS cylinders. The relaxation times of the normal mode process in both samples can be fitted to a single VFT equation and this implies PI-block relaxation on the same environment, which is in good agreement with the static picture (Figure 9) of polar aggregation only within the PS phase. A separate process due to macroscopic polarization effects known as the Maxwell–Wagner–Sillars (MWS) process[41] was not observed in our DS measurements. This low-frequency process appears in heterogeneous systems with strong polarization effects on the macroscopic scale which are caused by the differences in conductivity and permittivity of the components. Possible reasons for the absence of the MWS process are (i) the small volume fraction of the polar groups and (ii) the small size of aggregates (about 10 Å).

When the functional groups are placed on the PI chain end the dielectric response of the system becomes rich. In addition to the fast segmental and slow normal mode found in N-IS samples there is an intermediate process in all Zw-IS samples. A typical example is shown in Figure 14 where we plot the τ_{max} in an Arrhenius representation for the three processes in Zw-IS#4 and the two processes in N-IS#4 and bulk PI. The low-T relaxation is identified with the local segmental mode which is again indistinguishable between the dimethylamino- and zwitterion-substituted copolymers and conforms to the VFT equation with parameters log(τ_0/s) = −13, B = 600 K, and T_0 = 176 K. Furthermore, the distribution of relaxation times which is parametrized by the HN-shape parameters α and γ, assumes values typical for the segmental mode of bulk PI (α = 0.65, γ = 0.6). However, the segmental relaxation times are slower than those for the pure PI as a result of the slightly different microstructure and hence the higher T_g. The normal mode of N-IS#4 is considerably retarded compared to bulk PI, notwithstanding the dissolution of the microdomain structure with increasing T (Figure 3). There is also an indication for a slow process in Zw-IS#4 (○ in Figure 14) which probably corresponds to the Rouse dynamics of free (not associated) PI chains

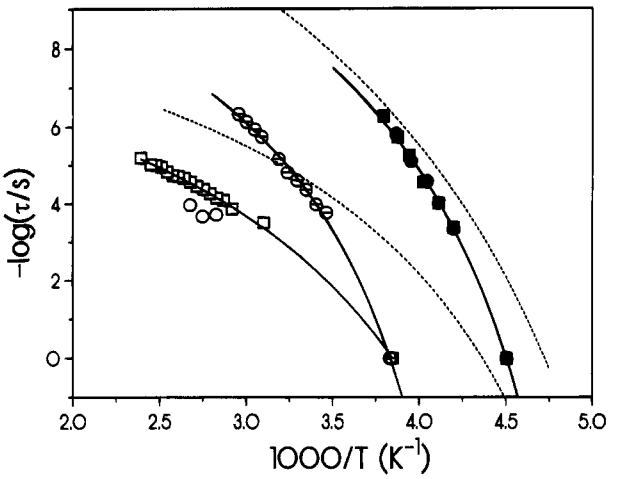

Figure 14. Arrhenius plot of the segmental (filled symbols), normal (open symbols), and intermediate process (⊖) in Zw-IS#4 (○, ●) in comparison with N-IS#4 (□, ■) and bulk PI (dashed lines).

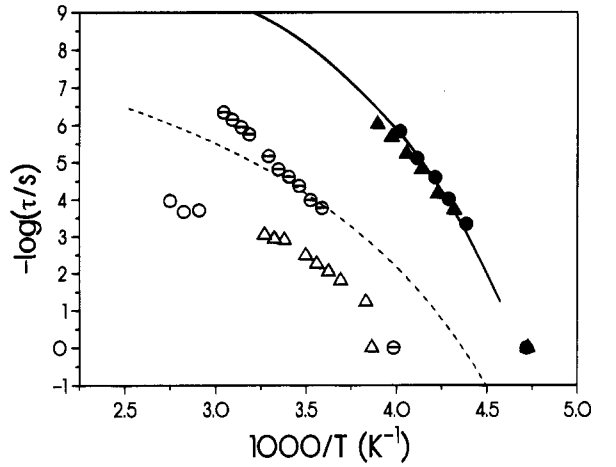

Figure 15. Arrhenius plot of the segmental (filled symbols), normal (open symbols), and intermediate process in Zw-IS#4 (●, ○, ⊖) and Zw-SI#4 (▲, △) under isofriction conditions (see text).

(Figure 9). The intermediate process in Zw-IS#4 (⊖ in Figure 14) is a new feature which deserves more attention. The relaxation strength for this process is similar to that for the segmental process, and fitting the T dependence of the relaxation times to the VFT equation reveals a similar activation energy (B = 614 K and T_0 = 204 K) with the segmental mode at lower T. This process is likely to originate from the regions of reduced mobility created around the polar aggregates which impend the motion of isoprene chains in their immediate environment. An intermediate T_g, however, could not be detected by DSC probably because of the small size of these regions compared to the typical resolution of this technique (≈100 Å).

The relaxation times of Zw-IS#4 and Zw-SI#4 are compared in Figure 15. For this comparison to be meaningful we have corrected for the difference in the local PI-like segmental friction. The results reveal that the intermediate process in Zw-IS#4 is not related to the PI normal mode since at high T it becomes even faster than the same process in bulk PI. The slow modes in Zw-SI#4 and Zw-IS#4 can be fitted to a single VFT equation which implies that they correspond to the normal mode on nonaggregated ("free") chains. The DS results, which are sensitive to both local and global

motions of the PI-block support the static picture (Figure 9) of nonassociated PI chains, at high T, in both Zw-SI and Zw-IS systems and of associated polar groups within the PI environment only at low T.

Conclusion

ω-Functionalized diblock copolymers of PS and PI constitute an ideal system to study the influence of the rich static structure on the local and global dynamics. The static picture consists of two separate levels of microphase separation, one between the two blocks forming the microdomain structure and another one between ionic and nonionic material. Although this kind of twin microphase separation has been observed earlier in different systems, it is the first time that it has been observed within the Q range of a single SAXS experiment. Because of the small difference in the dielectric constant of the two blocks, aggregates are consistently formed in the phase where the polar group is linked. Therefore, when the zwitterion is linked to the PI chain end, aggregates are formed at low temperatures within the PI phase. The aggregation shows up in rheology and dielectric spectroscopy with an extended rubbery plateau and with a new dielectric process associated with restricted PI segmental relaxation. At higher temperatures, the rheological response suggests a structure where the polar end groups are arranged between the PS cylinders with a liquid-like order.

When the zwitterion is located on the PS chain end, association takes place, at high temperatures, within the PS phase and stabilizes the new microdomain up to very high temperatures. In the near future we will explore in more detail the possibility of altering the phase behavior in diblock and triblock copolymers by introducing small polar groups at the different chain ends.

References and Notes

(1) Eisenberg, A. *Macromolecules* **1970**, *3*, 147.
(2) MacKnight, W. J.; Earnest, T. R. *J. Polym. Sci., Macromol. Rev.* **1981**, *16*, 41.
(3) Nyrkova, I. A.; Khokhlov, A. R.; Doi, M. *Macromolecules* **1993**, *26*, 3601.
(4) Nyrkova, I. A.; Khokhlov, A. R.; Doi, M. *Macromolecules* **1994**, *27*, 4220.
(5) Earnest, T. R.; Higgins, J. S.; Handlin, D. L.; MacKnight, W. J. *Macromolecules* **1981**, *14*, 192.
(6) Hird, B.; Eisenberg, A. *J. Polym. Sci., Polym. Phys.* **1990**, *28*, 1665.
(7) Douglas, E. D.; Waddon, A. J.; MacKnight, W. J. *Macromolecules* **1994**, *27*, 4344.
(8) Hodge, I. M.; Eisenberg, A. *Macromolecules* **1978**, *11*, 283.
(9) MacKnight, W. J.; Taggart, W. P.; Stein, R. S. *J. Polym. Sci., Polym. Symp.* **1974**, *45*, 113.
(10) Eisenberg, A.; Hird, B.; Moore, R. B. *Macromolecules* **1990**, *23*, 4098.
(11) Yarusso, D. J.; Cooper, S. L. *Macromolecules* **1983**, *16*, 1871.
(12) Williams, C. E.; Russell, T. P.; Jerome, R.; Horrion, J. *Macromolecules* **1986**, *19*, 2877.
(13) Register, R. A.; Cooper, S. L.; Thiyagarajan, P.; Chakrapani, S.; Jerome, R. *Macromolecules* **1990**, *23*, 2978.
(14) Gauthier, S.; Eisenberg, A. *Macromolecules* **1987**, *20*, 760.
(15) Weiss, R. A.; Sen, A.; Pottick, L. A.; Willis, C. L. *Polym. Commun.* **1990**, *31*, 221.
(16) Venkateshwaran, L. N.; York, G. A.; DePorter, C. D.; McGrath, J. E. *Polymer* **1992**, *33*, 2277.
(17) Lu, X.; Steckle, W. P.; Weiss, R. A. *Macromolecules* **1993**, *26*, 5876.
(18) Shen, Yi.; Satinya, C. R.; Fetters, L.; Adam, M.; Witten, T.; Hadjichristidis, N. *Phys. Rev. A* **1991**, *43*, 1886.
(19) Davidson, N. S.; Fetters, L. J.; Funk, W. G.; Graessley, W. W.; Hadjichristidis, N. *Macromolecules* **1988**, *21*, 112.
(20) Fetters, L. J.; Graessley, W. W.; Hadjichristidis, N.; Kiss, A. D.; Pearson, D. S.; Younghouse, L. B. *Macromolecules* **1988**, *21*, 1644.
(21) Pispas, S.; Hadjichristidis, N. *Macromolecules* **1994**, *27*, 1891.
(22) Pispas, S.; Hadjichristidis, N.; Mays, J. W. *Macromolecules* **1994**, *27*, 6307.
(23) Morton, M.; Fetters, L. *J. Rubber Chem. Technol.* **1975**, *48*, 359.
(24) Roovers, J.; Toporowski, P. *Macromolecules* **1983**, *16*, 843.
(25) Stewart, M. J.; Shepherd, N.; Service, D. *Br. Polym. J.* **1990**, *22*, 319.
(26) Eisenbach, C. D.; Schnecko, H.; Kern, W. *Polym. J.* **1975**, *11*, 699.
(27) Iatrou, H.; Hadjichristidis, N. *Macromolecules* **1992**, *25*, 4649.
(28) Iatrou, H.; Hadjichristidis, N. *Macromolecules* **1993**, *26*, 2479.
(29) Floudas, G.; Vogt, S.; Pakula, T.; Fischer, E. W. *Macromolecules* **1993**, *26*, 7210.
(30) Floudas, G.; Pakula, T.; Fischer, E. W.; Hadjichristidis, N.; Pispas, S. *Acta Polym.* **1994**, *45*, 176.
(31) Floudas, G.; Hadjichristidis, N.; Iatrou, H.; Pakula, T.; Fischer, E. W. *Macromolecules* **1994**, *27*, 7735.
(32) Fischer, E. W. *Physica A* **1993**, *201*, 183.
(33) Chu, B.; Wang, J.; Li, Y.; Peiffer, D. *Macromolecules* **1992**, *25*, 4229.
(34) Bates, F. S.; Rosedale, J. H.; Fredrickson, G. H. *J. Chem. Phys.* **1990**, *92*, 6255.
(35) Lu, X.; Steckle, W. P.; Hsiao, B.; Weiss, R. A. *Macromolecules* **1995**, *28*, 2831.
(36) Dobrynin, A. V.; Erukhimovich, I. Ya. *Macromolecules* **1993**, *26*, 276.
(37) Olvera de la Cruz, M.; Sanchez, I. C. *Macromolecules* **1986**, *19*, 2501.
(38) Stockmayer, W. H. *Pure Appl. Chem.* **1967**, *15*, 539.
(39) Adachi, K.; Kotaka, T. *Prog. Polym. Sci.* **1993**, *18*, 585.
(40) Doi, M.; Edwards, S. F. *The Theory of Polymer Dynamics*; Clarendon Press: Oxford, U.K., 1986.
(41) Steeman, P. A. M. Ph.D. Thesis, Delft University, 1992.

MA950042L